On data association with possibly unresolved measurements

Augustin A Saucan, Florian Meyer

On Data Association with Possibly Unresolved Measurements

Augustin A. Saucan
Télécom SudParis
Institut Polytechnique de Paris
Paris, France
augustin.saucan@telecom-sudparis.eu

Florian Meyer
Scripps Institution of Oceanography
Department of Electrical and Computer Engineering
University of California San Diego
San Diego, CA
flmeyer@ucsd.edu

***Abstract*—Tracking targets based on measurements provided by radar, sonar, or lidar sensors is essential to obtain situational awareness in important applications, including autonomous navigation and applied ocean sciences. A key challenge in multitarget tracking is the unknown association between the available measurements and the targets to be tracked. In particular, robust data association for closely spaced targets requires advanced methods that explicitly model unresolved measurements. Due to limited sensor resolution, the sensor produces a single measurement for two or more actual targets. If not explicitly modeled in the multitarget tracking method, unresolved measurements lead to track losses and thus, to significant tracking errors. In this paper, we propose a scalable data association method for the tracking of multiple potentially unresolved targets. A loopy belief propagation method is presented that efficiently approximates the marginal association probabilities given a set of potentially unresolved measurements. This method scales quadratically in the number of targets and linearly in the number of measurements. Our numerical results demonstrate that the computed approximate marginal association probabilities are close in L_1 distance to the true marginal association probabilities, which can only be calculated for very small tracking scenarios.**

I. Introduction

Tracking multiple targets [1]–[8] in densely packed scenarios is of high interest in many areas of engineering, such as autonomous navigation, applied ocean sciences, air traffic control, and biomedical analysis. Due to limited sensor resolution, closely spaced targets may become unresolved, and only a single measurement is perceived for the entire group of targets by the respective sensor. Such scenarios pose difficulties and often lead to lost tracks when unresolved targets are not explicitly considered.

A. Existing Methods

There exist several tracking approaches that consider multitarget tracking with potentially unresolved measurements. Several methodologies for tracking two crossing targets from imaging sensors are presented in [1, Ch.9.4]. From each frame, a segmentation method extracts a small image ("hot spot") corresponding to either one target or an unresolved pair of targets that overlaps. The segmentation method also detects potential overlap. When overlapping is detected, several measurements are collected: a single merged measurement for the centroid of the overlapping hot spot and two displacement measurements between the two targets with an ambiguous origin. The merged centroid is assumed to be a linear combination of the individual target images, where the mixing coefficient is determined based on their relative pixel intensities. Before overlapping, the two targets are tracked using separate filters. When overlapping is detected, tracking switches to coupled filtering using a stacked state vector. Two variants of coupled Joint Probabilistic Data Association Filter (JPDAF) are proposed for filtering during the overlapping period.

In [9], [10] and [1, Ch.6.4], a fixed-grid resolution model is employed to determine when two targets are unresolved. Subsequently, the joint probabilities for two targets and their corresponding association hypotheses are derived, followed by Gaussian approximations for the target state's marginal probability density functions (pdfs). The proposed methodology of [9], [10], named Joint Probabilistic Data Association with Merged Measurements (JPDAM), was improved in [11] by proposing a simpler approximation to the pdf of the merged measurement.

As opposed to the fixed-grid model of [9]–[11], in [12], a sensor model is proposed where the resolution capability is determined by a conditional probability of the event that two targets are unresolved. Tracking two possibly unresolved targets is addressed via a generalization of Multiple Hypothesis Tracking (MHT) that considers the added hypotheses of unresolved targets with the proposed model. This same resolution model is also employed by the authors of [13], which further propose an Interacting Multiple Models (IMM)-JPDAM technique to account for maneuvering targets as well as for unresolved measurements.

Using analytic combinatorics, the authors of [14] propose a joint-likelihood function that incorporates all the feasible hypotheses regarding the measurements and the targets. Subsequently, the authors propose a Joint Probabilistic Data Association (JPDA) filter for a two-target tracking scenario. In [15], the sensor resolution capabilities are translated into resolution events, where each event is a partitioning of the targets into groups–each group being unresolved. To evaluate the probability of each such event, resolution graphs are introduced, where targets represent nodes, and bidirectional

edges represent unresolved pairs of targets. A connected subgraph represents a group of unresolved targets. Each edge has a corresponding probability that the two targets are unresolved, which has the same expression as in [12]. Thus, the model of [15] can be seen as an extension of the two-target model [12] to the case of a fixed number of multiple targets. The joint posterior pdf of targets is obtained in [15] by marginalizing over all feasible resolution graphs and all feasible associations for each graph. Gaussian mixture and single-Gaussian approximate filters are also provided.

An labeled random finite set (LRFS)-based multitarget tracking filter with merged measurements was proposed in [4] by relying on a generalized labeled multi-Bernoulli (GLMB) to model the multiple targets coupled with a generic merged-measurement model. The GLMB model is a weighted mixture of different LRFSs, called hypotheses, and the GLMB filter [7] sequentially propagates these hypotheses via prediction and update. The disadvantage of GLMB filters, including [4], is given by the exponential increase over time of the number of hypotheses. A merged measurement labeled multi-Bernoulli (LMB) filter is proposed in [16] and alleviates the growth mentioned above of hypotheses over time, however still retains the need to construct and evaluate numerous association hypotheses during the update procedure, followed by a direct marginalization for each target across these hypotheses.

B. Contribution

In this paper, we address the case of tracking a fixed number of targets where any two targets can become unresolved. Within this "Unresolved Two-Target (UTT)" model, we determine the probability of all target pairs becoming an unresolved pair using an expression borrowed from [12]. Here, knowledge of the sensor resolution capabilities and the distance between the state vectors of the two targets are considered. A resolution graph describes a resolution event where the nodes are the targets. There is an edge between nodes if targets contribute to the same unresolved measurement. We constrain the maximum degree of the graph to be at most one to ensure that there are at most two targets that contribute to an unresolved measurement.

In contrast to the approaches mentioned above, our proposed method relies on message passing and, more specifically, on the Loopy Belief Propagation (LBP) [3], [6], [17], [18] to efficiently approximate marginal pdfs of the target state. To achieve this, a set of association variables are defined, allowing for the factorization of the posterior multitarget pdf, and an LBP algorithm is tailored to the resulting factor graph. The proposed LBP method for the UTT model scales quadratically with the number of targets and linearly with the number of measurements.

Notation: Throughout this work, the following notations are employed. Random variables are displayed in sans serif, upright fonts; their realizations in serif, italic fonts. Vectors and matrices are denoted by bold lowercase and uppercase letters, respectively. Random sets and their realizations are denoted by upright sans serif and calligraphic font, respectively. For example, a random vector and its realization are denoted by $\mathbf{x}$ and $\boldsymbol{x}$ while a random set and its realization are denoted by X and $\mathcal{X}$, respectively. The set cardinality is denoted by $|\mathsf{X}|$. The set of integers $\{a, a+1, \cdots, b\}$, for any $a < b$, is denoted as $[\![a, b]\!]$. Equality up to a normalization factor is denoted as $\propto$.

II. The Proposed UTT Model

We consider a number of n_{o} randomly maneuvering targets. The trajectory of each target $i \in [\![1, n_{\mathrm{o}}]\!]$ is characterized by a stochastic process $\mathbf{x}_k^{(i)} \in \mathbb{R}^d$. At each discrete time step, indexed by k, the multitarget state is obtained by concatenating the individual state vectors as $\mathbf{x}_k = \big[(\mathbf{x}_k^{(1)})^\top, (\mathbf{x}_k^{(2)})^\top, \cdots, (\mathbf{x}_k^{(n_{\mathrm{o}})})^\top\big]^\top$. Measurements performed at time k are denoted as $\mathbf{z}_k$ and the joint vector of all measurements collected up to time k as $\mathbf{z}_{1:k}$. It is assumed that we are at time k, and the predicted posterior pdf, $f(\boldsymbol{x}_k|\boldsymbol{z}_{1:k-1})$, is available. Furthermore, it is assumed that this pdf factorizes as

$$f(\boldsymbol{x}_k|\boldsymbol{z}_{1:k-1}) = \prod_{i=1}^{n_{\mathrm{o}}} f\big(\boldsymbol{x}_k^{(i)}|\boldsymbol{z}_{1:k-1}\big). \tag{1}$$

In what follows, the UTT measurement model is presented where any two targets with indexes in $[\![1, n_{\mathrm{o}}]\!]$ can potentially generate a single unresolved measurement—in which case, we will refer to the two targets as unresolved. The UTT model generalizes the model of [12], the latter only treating the case where $n_{\mathrm{o}} = 2$.

We define an UTT resolution event $\mathcal{R}$ as a set $\mathcal{R} = \big\{\mathcal{R}_1, \cdots, \mathcal{R}_N\big\}$ with $|\mathcal{R}_n| \leq 2$, $n \in \{1, \ldots, N\}$ that partitions $[\![1, n_{\mathrm{o}}]\!]$, i.e., $\cup_{i=1}^{N} \mathcal{R}_i = [\![1, n_{\mathrm{o}}]\!]$. In particular, each element in $\mathcal{R}$ is either a singleton or a tuple; in the latter, the tuple contains the indices of two unresolved targets, while in the former, it contains the index of a resolved target. Moreover, all elements in $\mathcal{R}$ are disjoint, and their union yields $[\![1, n_{\mathrm{o}}]\!]$. We introduce the set of all such resolution events as $\mathcal{P}_2$. Note that here, the subscript 2 denotes that the resolution event consists of sets with at most two target indices.

The probability that targets with indexes $i, l \in [\![1, n_{\mathrm{o}}]\!]$ form an unresolved pair and generate an unresolved measurement is modeled as [12]

$$P_{\mathrm{u}}(\boldsymbol{x}_k^{(i)}, \boldsymbol{x}_k^{(l)}) = \exp\Big(-\frac{1}{2}(\Delta_k^{il})^\top (\boldsymbol{A}_{\mathrm{u}})^{-1}\, \Delta_k^{il}\Big).$$

Here, $\boldsymbol{A}_{\mathrm{u}}$ is a positive definite matrix that describes the resolution capabilities of the sensor. We also introduced $\Delta_k^{il} \triangleq \boldsymbol{h}_{\mathrm{r}}(\boldsymbol{x}_k^{(i)}) - \boldsymbol{h}_{\mathrm{r}}(\boldsymbol{x}_k^{(l)})$, where $\boldsymbol{h}_{\mathrm{r}}(\cdot)$ is the measurement model of the sensor for the resolved target case. If two targets are close in the measurement domain, they yield a small Δ_k^{il} and thus a high probability, $P_{\mathrm{u}}(\boldsymbol{x}_k^{(i)}, \boldsymbol{x}_k^{(l)})$, that they generate an unresolved measurement. A discussion on typical values for the resolution matrix $\boldsymbol{A}_{\mathrm{u}}$ is provided in [12].

Conditioned on the multitarget state $\mathbf{x}_k$, the probability of an UTT resolution event $\mathsf{R} = \mathcal{R}$, with $\mathcal{R} \in \mathcal{P}_2$, is obtained as

$$p(\mathcal{R}|\boldsymbol{x}_k) = V_{\mathrm{u}}(\boldsymbol{x}_k) \prod_{\{i,l\}\in\mathcal{R}} \frac{P_{\mathrm{u}}\big(\boldsymbol{x}_k^{(i)}, \boldsymbol{x}_k^{(l)}\big)}{1 - P_{\mathrm{u}}\big(\boldsymbol{x}_k^{(i)}, \boldsymbol{x}_k^{(l)}\big)}. \tag{2}$$

Here, $\prod_{\{i,l\}\in\mathcal{R}}$ denotes the product over all sets $\mathcal{R}_n \in \mathcal{R}$ with $|\mathcal{R}_n| = 2$ and $V_{\mathrm{u}}(\boldsymbol{x}_k)$ is a normalization constant, i.e.,

$$V_{\mathrm{u}}(\boldsymbol{x}_k) \triangleq \Bigg(\sum_{\mathcal{R}\in\mathcal{P}_2} \prod_{\{i,l\}\in\mathcal{R}} \frac{P_{\mathrm{u}}\big(\boldsymbol{x}_k^{(i)}, \boldsymbol{x}_k^{(l)}\big)}{1 - P_{\mathrm{u}}\big(\boldsymbol{x}_k^{(i)}, \boldsymbol{x}_k^{(l)}\big)} \Bigg)^{-1}. \quad (3)$$

A resolution event $\mathcal{R} \in \mathcal{P}_2$ can be seen as a random undirected graph with a set of vertices $[\![1, n_{\mathrm{o}}]\!]$ and a set of edges $\mathcal{R}$. The restriction $\mathcal{R} \in \mathcal{P}_2$ is equivalent to imposing that the maximum degree of the graph is strictly less than 2.

At time k, m_k measurements are collected, i.e., $\mathbf{z}_k^{(j)} \in \mathbb{Z}$, $j \in \{1, \ldots, \mathsf{m}_k\}$. Note that the number of measurements, m_k, is also random. Given a resolution event $\mathcal{R}$, each element in $\mathcal{R}_n \in \mathcal{R}$ may produce a target-originated measurement vector. In addition to target-generated measurements, there are also clutter-generated measurements. A detailed description of the proposed UTT target detection and measurement model is provided next.

- For each singleton $\{i\} \in \mathcal{R}$, the corresponding resolved target can generate up to one measurement. More specifically, with probability $P_{\mathrm{d}}^{(i)}$, the i-th target with state vector $\boldsymbol{x}_k^{(i)}$ generates a measurement vector according to
$$\mathbf{z}_k^{(j)} = \boldsymbol{h}_{\mathrm{r}}(\mathbf{x}_k^{(i)}) + \mathbf{v}_k^{(j)} \quad (4)$$
where $\mathbf{v}_k^{(j)} \sim \mathcal{N}(\mathbf{0}, \boldsymbol{R})$ is the corresponding measurement noise. From (4), we can directly get the resolved target likelihood function $f\big(\boldsymbol{z}_k^{(j)} | \boldsymbol{x}_k^{(i)}\big)$. With probability $1 - P_{\mathrm{d}}^{(i)}$, the i-th target is undetected, and no measurement is generated. This is typically referred to as missed detection. The detection procedure is carried out independently for every resolved target, i.e., for every $\{i\} \in \mathcal{R}$.
- For each $\{i, l\} \in \mathcal{R}$, the corresponding pair of unresolved targets generates a single unresolved measurement according to
$$\mathbf{z}_k^{(j)} = \boldsymbol{h}_{\mathrm{u}}\big(\mathbf{x}_k^{(i)}, \mathbf{x}_k^{(l)}\big) + \mathbf{v}_k^{(j)} \quad (5)$$
where $\boldsymbol{h}_{\mathrm{u}}\big(\mathbf{x}_k^{(i)}, \mathbf{x}_k^{(l)}\big)$ is the merged measurement model [e.g., $\boldsymbol{h}_{\mathrm{u}}(\boldsymbol{x}, \boldsymbol{y}) = \frac{1}{2}(\boldsymbol{h}_{\mathrm{r}}(\boldsymbol{x}) + \boldsymbol{h}_{\mathrm{r}}(\boldsymbol{y}))$] and $\mathbf{v}_k^{(j)} \sim \mathcal{N}(\mathbf{0}, \boldsymbol{R}_{\mathrm{u}})$ is again measurement noise. Here, a single target-originated measurement is always generated, i.e., any unresolved pair of targets is always detected. From (5), we can directly get the unresolved targets likelihood function $f\big(\boldsymbol{z}_k^{(j)} | \boldsymbol{x}_k^{(i)}, \boldsymbol{x}_k^{(l)}\big)$.
- Clutter-generated measurements are independent and identically distributed (iid) with pdf $f_{\mathrm{c}}(\boldsymbol{z}^{(j)})$. The number of clutter measurements follows a Poisson distribution with rate parameter λ_{c} [1].

The measurement noise $\mathbf{v}_k^{(j)}$ in (4) and (5) is assumed independent across index j and independent of clutter-originated measurements. Both clutter and target-originated measurements are arranged in a concatenated measurement vector, $\mathbf{z}_k = \big[(\mathbf{z}_k^{(1)})^\top, \cdots, (\mathbf{z}_k^{(\mathsf{m}_k)})^\top\big]^\top$. The order of measurements in this vector is random. We assume *measurement origin uncertainty*, i.e., the origin—whether single target, pair of targets, or clutter—of a single measurement $\mathbf{z}_k^{(j)}$ is unknown.

Remark 1. *Note the difference between the UTT model introduced in this paper and the one presented in [12]. A pair of unresolved targets, in the former, always generates an unresolved measurement while, in the latter, it may or may not generate a measurement. For example, under the model of [12], an ambiguity arises when all measurements are clutter. Namely, the unresolved and undetected event becomes indistinguishable from the resolved and undetected event. Within our model, the case where all measurements are clutter-originated is represented by a single resolution event, i.e., the event $\mathcal{R}$ where for all $\mathcal{R}_n \in \mathcal{R}$ we have $|\mathcal{R}_n| = 1$. This is because, here, a pair of unresolved targets implies that both targets have been detected, but only a single measurement is generated due to limited sensor resolution. On the other hand, following the model in [12], multiple resolution events can represent the aforementioned "all-clutter" case.*

III. Statistical Model and Problem Formulation

In what follows, we will present the statistical model for data association with potentially unresolved targets.

A. Data Association Vectors and Constraints

Due to unresolved measurements, measurement-origin uncertainty, and clutter measurements, there exist a large number of possible explanations for the observed measurement vector $\boldsymbol{z}_k = \big[(\boldsymbol{z}_k^{(1)})^\top, \cdots, (\boldsymbol{z}_k^{(m_k)})^\top\big]^\top$. This fact is represented by the random target-oriented association vector $\mathbf{a}_k = [\mathsf{a}_k^{(1)}, \cdots, \mathsf{a}_k^{(n_{\mathrm{o}})}]^\top$ with entries

$$\mathsf{a}_k^{(i)} = \begin{cases} j \in [\![1, m_k]\!] & \text{target } i \text{ generated/contributed to} \\ & \text{the } j\text{-th measurement} \\ 0 & \text{target } i \text{ has not contributed to} \\ & \text{to any measurement.} \end{cases}$$

Note that not every $\boldsymbol{a}_k \in \mathcal{A}_k \triangleq [\![0, m_k]\!]^{n_{\mathrm{o}}}$ is valid. In particular, an $\boldsymbol{a}_k \in \mathcal{A}_k$ is invalid if it describes an event where a measurement has contributions from more than two targets. The validity of an event can thus be verified by evaluating the following binary constraint, i.e.,

$$\Psi_k(\boldsymbol{a}_k) = \begin{cases} 0, & \exists i, j, l \in [\![1, n_{\mathrm{o}}]\!] \\ & \text{s.t. } a_k^{(i)} = a_k^{(j)} = a_k^{(l)} \neq 0 \\ 1, & \text{otherwise.} \end{cases} \quad (6)$$

If we knew the valid $\boldsymbol{a}_k$ that generated the measurement vector $\boldsymbol{z}_k$, we could explain the origin of every measurement and, at the same time, unambiguously specify the target resolution event $\mathcal{R}$. However, $\mathbf{a}_k$ is random and thus a nuisance parameter in our Bayesian state estimation problem. For minimum mean squared error estimation, nuisance parameters are marginalized by computing a marginal posterior pdf from a joint posterior pdf. Within this marginalization step, for each possible multitarget state vector $\boldsymbol{x}_k$, a sum with a number of terms that is equal to all possible association vectors $\boldsymbol{a}_k$ needs to be computed. Due to the large number of possible vectors, this is typically infeasible.

As in [3], [6], [17], we aim to develop a feasible approximate target state estimation based on LBP. Here, the aforementioned infeasible marginalization is avoided by introducing the complementary measurement-oriented association vector $\mathbf{b}_k = [\mathbf{b}_k^{(1)}, \mathbf{b}_k^{(2)}, \cdots, \mathbf{b}_k^{(m_k)}]^\top$, where each entry $\mathbf{b}_k^{(j)} = \left[\mathsf{b}_{k,1}^{(j)}, \mathsf{b}_{k,2}^{(j)}\right]^\top$ specifies the origin of a measurement, i.e.,

$$\mathbf{b}_k^{(j)} = \begin{cases} [i,i] & \text{the } j\text{-th measurement was generated by target } i \in [\![1, n_\mathrm{o}]\!] \\ [i,l] & \text{the } j\text{-th measurement was generated by targets } i,l \in [\![1, n_\mathrm{o}]\!],\ i > l \\ [0,0] & \text{the } j\text{-th measurement was generated by clutter.} \end{cases}$$

Here, each entry in $\mathbf{b}_k$ is a tuple $[i,l]$ with elements that are decreasingly ordered. A measurement-oriented association vectors is an element of $\mathcal{B}_k \triangleq \mathcal{B}^{m_k}$, where $\mathcal{B} = \left\{[i,l] : i,l \in [\![1, n_\mathrm{o}]\!] \text{ and } i > l\right\} \cup \left\{[0,0]\right\}$. However, not all vectors in $\mathcal{B}_k$ are valid measurement-oriented association vectors. An event is invalid if a target contributes to more than one measurement. Validity can be checked by introducing a constraint for target-oriented association vectors. We skip this step here for the sake of brevity.

For each valid $\boldsymbol{a}_k$, there is exactly one valid $\boldsymbol{b}_k$ and vice versa. For example, in the all-clutter case, the measurement-oriented association vectors defined by $\boldsymbol{b}_k^{(j)} = [0,0],\ \forall j$, uniquely corresponds to $\boldsymbol{a}_k = [0, \cdots, 0]^\top$. It can easily be verified that for invalid $\boldsymbol{a}_k$ and $\boldsymbol{b}_k$, however, there does not exist a corresponding invalid $\boldsymbol{b}_k$ and $\boldsymbol{a}_k$, respectively. For example, an invalid event where three targets contribute to the same measurement can be described by an $\boldsymbol{a}_k \in \mathcal{A}_k$ but not by a $\boldsymbol{b}_k \in \mathcal{B}_k$.

We can check if a $\boldsymbol{a}_k$ and $\boldsymbol{b}_k$ represent the same association event by introducing the following product of elementwise consistency constraints, i.e.,

$$\Psi_k(\boldsymbol{a}_k, \boldsymbol{b}_k) = \prod_{i=1}^{n_\mathrm{o}} \prod_{j=1}^{m_k} \psi_{ij}(a_k^{(i)}, \boldsymbol{b}_k^{(j)}) \tag{7}$$

with

$$\psi_{ij}(a_k^{(i)}, \boldsymbol{b}_k^{(j)}) = \begin{cases} 0, & a_k^{(i)} = j \text{ and } \nexists q \text{ s.t. } b_{k,q}^{(j)} = i \\ & \text{or } \exists q \text{ s.t. } b_{k,q}^{(j)} = i \text{ and } a_k^{(i)} \neq j \\ 1, & \text{otherwise}\,. \end{cases} \tag{8}$$

Only if all elements in $\boldsymbol{a}_k$ are consistent with all elements in $\boldsymbol{b}_k$, i.e., all elementwise consistency constraints in (7) are equal to one, the two vectors represent the same association event. Since only valid events can be represented by an $\boldsymbol{a}_k$ and a $\boldsymbol{b}_k$ at the same time, the represented event must be valid.

By also introducing a measurement-oriented association vector $\mathbf{b}_k$, we can thus replace the constrain that is a function of the high-dimensional vector $\boldsymbol{a}_k$ in (6), by multiple constraints that are a function of low-dimensional vectors and scalars in (7). This step is critical for feasible data association using LBP.

B. The Joint Posterior Pdf

The goal of this paper is to compute marginal association probabilities, $p(\boldsymbol{b}_k^{(j)}|\boldsymbol{z}_{1:k})$, for each measurement $j \in [\![1, m_k]\!]$. In principle, these marginal probability mass functions (pmfs) can be obtained from the joint posterior pdf $f(\boldsymbol{x}_k, \boldsymbol{a}_k, \boldsymbol{b}_k|\boldsymbol{z}_{1:k})$, which involves the target states and all association variables at time k, by direct marginalization. However, this is typically infeasible due to the large number of valid association events. To obtain feasible estimates of the required marginals, i.e., $\hat{p}_j(\boldsymbol{b}_k^{(j)}|\boldsymbol{z}_{1:k})$, $j \in [\![1, m_k]\!]$, we apply LBP on the factor graph representing $f(\boldsymbol{x}_k, \boldsymbol{a}_k, \boldsymbol{b}_k|\boldsymbol{z}_{1:k})$ [19].

In what follows, we assume that the measurement at time k, $\boldsymbol{z}_k$, has been observed and is thus fixed. Note that this implies that m_k is also observed and fixed. By using Bayes' rule, the joint posterior factorizes as

$$\begin{aligned} f(\boldsymbol{x}_k, \boldsymbol{a}_k, \boldsymbol{b}_k|\boldsymbol{z}_{1:k}) &= f(\boldsymbol{x}_k, \boldsymbol{a}_k, \boldsymbol{b}_k|\boldsymbol{z}_{1:k-1}, \boldsymbol{z}_k, m_k) \\ &\propto f(\boldsymbol{z}_k|\boldsymbol{x}_k, \boldsymbol{a}_k, \boldsymbol{b}_k, m_k) p(\boldsymbol{a}_k, \boldsymbol{b}_k|\boldsymbol{x}_k, m_k) \\ &\quad \times f(\boldsymbol{x}_k|\boldsymbol{z}_{1:k-1}). \end{aligned} \tag{9}$$

Note that here we have made the common assumption [6] that, conditioned on $\boldsymbol{x}_k$ and m_k, the association vectors $\boldsymbol{a}_k$ and $\boldsymbol{b}_k$ are independent of all previous measurements $\boldsymbol{z}_{1:k-1}$.

The first term in (9) corresponds to the likelihood of the measurement $\boldsymbol{z}_k$ that, based on the assumptions discussed in Section II, can be written as

$$\begin{aligned} f(\boldsymbol{z}_k|\boldsymbol{x}_k, \boldsymbol{a}_k, \boldsymbol{b}_k, m_k) &= f(\boldsymbol{z}_k|\boldsymbol{x}_k, \boldsymbol{b}_k, m_k) \\ &= \left[\prod_{j=1}^{m_k} f_\mathrm{c}(\boldsymbol{z}_k^{(j)})\right] \prod_{j=1}^{m_k} g\big(\boldsymbol{x}_k, \boldsymbol{b}_k^{(j)}; \boldsymbol{z}_k^{(j)}\big). \end{aligned} \tag{10}$$

Here, we have introduced

$$\begin{aligned} g\big(\boldsymbol{x}_k, \boldsymbol{b}_k^{(j)}; \boldsymbol{z}_k^{(j)}\big) = &\prod_{l=1}^{n_\mathrm{o}} g_1^{(l)}\big(\boldsymbol{x}_k^{(l)}, \boldsymbol{b}_k^{(j)}; \boldsymbol{z}_k^{(j)}\big) \\ &\times \prod_{i=l+1}^{n_\mathrm{o}} g_2^{(il)}\big(\boldsymbol{x}_k^{(i)}, \boldsymbol{x}_k^{(l)}, \boldsymbol{b}_k^{(j)}; \boldsymbol{z}_k^{(j)}\big) \end{aligned}$$

with factors $g_1(\cdot)$ and $g_2(\cdot)$ defined as

$$g_1^{(l)}\big(\boldsymbol{x}_k^{(l)}, \boldsymbol{b}_k^{(j)}; \boldsymbol{z}_k^{(j)}\big) \triangleq \begin{cases} \frac{f(\boldsymbol{z}_k^{(j)}|\boldsymbol{x}_k^{(l)})}{f_\mathrm{c}(\boldsymbol{z}_k^{(j)})}, & \text{if } \boldsymbol{b}_k^{(j)} = [l,l] \\ 1, & \text{otherwise} \end{cases}$$

and

$$g_2^{(il)}\big(\boldsymbol{x}_k^{(i)}, \boldsymbol{x}_k^{(l)}, \boldsymbol{b}_k^{(j)}; \boldsymbol{z}_k^{(j)}\big) \triangleq \begin{cases} \frac{f(\boldsymbol{z}_k^{(j)}|\boldsymbol{x}_k^{(i)}, \boldsymbol{x}_k^{(l)})}{f_\mathrm{c}(\boldsymbol{z}_k^{(j)})}, & \text{if } \boldsymbol{b}_k^{(j)} = [i,l] \\ 1, & \text{otherwise.} \end{cases}$$

Let $\mathcal{M}_{\boldsymbol{b}_k}^\mathrm{u} = \{j \in [\![1, m_k]\!] \colon b_{k,1}^{(j)} \neq b_{k,2}^{(j)}\}$ denote the set of measurement indices that result from unresolved targets. In contrast, $\mathcal{M}_{\boldsymbol{b}_k}^\mathrm{r} = \{j \in [\![1, m_k]\!] \colon b_{k,1}^{(j)} = b_{k,2}^{(j)} \neq 0\}$ is the set of measurement indices that correspond to resolved and

detected targets. Furthermore, $\mathcal{M}_{\boldsymbol{b}_k} = \mathcal{M}^{\mathrm{u}}_{\boldsymbol{b}_k} \cup \mathcal{M}^{\mathrm{r}}_{\boldsymbol{b}_k}$ is the set of all target-generated measurements. Based on assumptions discussed in Section II and by using (2), the prior pmf of association vectors $\boldsymbol{a}_k \in \mathcal{A}_k$ and $\boldsymbol{b}_k \in \mathcal{B}$, can be obtained as

$$\begin{aligned} &p(\boldsymbol{a}_k, \boldsymbol{b}_k | \boldsymbol{x}_k, m_k) \\ &= V_{\mathrm{u}}(\boldsymbol{x}_k)\, \Psi_k(\boldsymbol{a}_k, \boldsymbol{b}_k)\, \frac{e^{-\lambda_{\mathrm{c}}} (\lambda_{\mathrm{c}})^{m_k - |\mathcal{M}_{\boldsymbol{b}_k}|}}{m_k!} \\ &\quad \times \left[\prod_{i=1}^{n_{\mathrm{o}}} \left(1 - P_{\mathrm{d}}^{(i)}\right) \right] \left[\prod_{j' \in \mathcal{M}^{\mathrm{r}}_{\boldsymbol{b}_k}} \frac{P_{\mathrm{d}}^{(j'_1)}}{1 - P_{\mathrm{d}}^{(j'_1)}} \right] \\ &\quad \times \prod_{j \in \mathcal{M}^{\mathrm{u}}_{\boldsymbol{b}_k}} \frac{Q_{\mathrm{u}}\left(\boldsymbol{x}_k^{(j_1)}, \boldsymbol{x}_k^{(j_2)}\right)}{\left(1 - P_{\mathrm{d}}^{(j_1)}\right)\left(1 - P_{\mathrm{d}}^{(j_2)}\right)} \end{aligned} \tag{11}$$

where we used the short notation $j_1 \triangleq b_{k,1}^{(j)}$, $j_2 \triangleq b_{k,2}^{(j)}$, and $Q_{\mathrm{u}}\big(\boldsymbol{x}_k^{(i)}, \boldsymbol{x}_k^{(l)}\big) \triangleq P_{\mathrm{u}}\big(\boldsymbol{x}_k^{(i)}, \boldsymbol{x}_k^{(l)}\big) / \big(1 - P_{\mathrm{u}}\big(\boldsymbol{x}_k^{(i)}, \boldsymbol{x}_k^{(l)}\big)\big)$. A detailed derivation of this expression will be provided in future work.

By plugging expressions in (1), (10), and (11) into (9), and dropping constant factors, we obtain

$$\begin{aligned} &f(\boldsymbol{x}_k, \boldsymbol{a}_k, \boldsymbol{b}_k | \boldsymbol{z}_{1:k}) \\ &\quad \propto V_{\mathrm{u}}(\boldsymbol{x}_k) \left[\prod_{i=1}^{n_{\mathrm{o}}} f\big(\boldsymbol{x}_k^{(i)} | \boldsymbol{z}_{1:k-1}\big) \right] \\ &\quad \times \prod_{j=1}^{m_k} \prod_{l=1}^{n_{\mathrm{o}}} \psi_{lj}\big(a_k^{(l)}, \boldsymbol{b}_k^{(j)}\big)\, q_1^{(l)}\big(\boldsymbol{x}_k^{(l)}, \boldsymbol{b}_k^{(j)}; \boldsymbol{z}_k^{(j)}\big) \\ &\quad \times \prod_{i=l+1}^{n_{\mathrm{o}}} q_2^{(il)}\big(\boldsymbol{x}_k^{(i)}, \boldsymbol{x}_k^{(l)}, \boldsymbol{b}_k^{(j)}; \boldsymbol{z}_k^{(j)}\big). \end{aligned} \tag{12}$$

Note that here we have introduced the combined factors

$$q_1^{(l)}\big(\boldsymbol{x}_k^{(l)}, \boldsymbol{b}_k^{(j)}; \boldsymbol{z}_k^{(j)}\big) \triangleq \begin{cases} \frac{P_{\mathrm{d}}^{(l)} f\left(\boldsymbol{z}_k^{(j)} \middle| \boldsymbol{x}_k^{(l)}\right)}{(1 - P_{\mathrm{d}}^{(l)}) \lambda_{\mathrm{c}} f_{\mathrm{c}}\left(\boldsymbol{z}_k^{(j)}\right)}, & \text{if } \boldsymbol{b}_k^{(j)} = [l, l] \\ 1, & \text{otherwise} \end{cases}$$

and

$$\begin{aligned} &q_2^{(il)}\big(\boldsymbol{x}_k^{(i)}, \boldsymbol{x}_k^{(l)}, \boldsymbol{b}_k^{(j)}; \boldsymbol{z}_k^{(j)}\big) \\ &\quad \triangleq \begin{cases} \frac{f\left(\boldsymbol{z}_k^{(j)} \middle| \boldsymbol{x}_k^{(i)}, \boldsymbol{x}_k^{(l)}\right) Q_{\mathrm{u}}\left(\boldsymbol{x}_k^{(i)}, \boldsymbol{x}_k^{(l)}\right)}{(1 - P_{\mathrm{d}}^{(i)})(1 - P_{\mathrm{d}}^{(l)})\, \lambda_{\mathrm{c}} f_{\mathrm{c}}\left(\boldsymbol{z}_k^{(j)}\right)}, & \text{if } \boldsymbol{b}_k^{(j)} = [i, l] \\ 1, & \text{otherwise.} \end{cases} \end{aligned}$$

The factorization structure of $f(\boldsymbol{x}_k, \boldsymbol{a}_k, \boldsymbol{b}_k | \boldsymbol{z}_{1:k})$ in (12) is key for the development of a scalable LBP method presented next.

IV. The Proposed LBP Algorithm

Before we develop the LBP message passing for the calculation of approximate marginal pdfs, we drop the factor $V_{\mathrm{u}}(\boldsymbol{x}_k)$, defined in (3), because it prohibits a factorization of (12) in the n_{o} target states. Dropping this factor is equivalent to approximating it by a constant. After dropping $V_{\mathrm{u}}(\boldsymbol{x}_k)$, we can represent (12) by the factor graph shown in Fig. 1. This

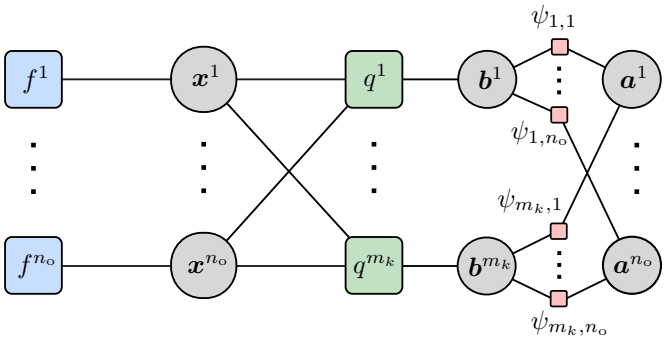

Fig. 1. Factor graph for the UTT model showcasing the dependencies between target state variables and association variables at a single time step k. The following compact notation was used: $f^i \triangleq f(\boldsymbol{x}_k^{(i)} | \boldsymbol{z}_{1:k-1})$, $\psi_{ij} \triangleq \psi_{ij}(a_k^{(i)}, \boldsymbol{b}_k^{(j)})$, and $q^j \triangleq \prod_{l=1}^{n_{\mathrm{o}}} q_1^{(l)}(\boldsymbol{x}_k^{(l)}, \boldsymbol{b}_k^{(j)}; \boldsymbol{z}_k^{(j)}) \prod_{i=l+1}^{n_{\mathrm{o}}} q_2^{(il)}(\boldsymbol{x}_k^{(i)}, \boldsymbol{x}_k^{(l)}, \boldsymbol{b}_k^{(j)}; \boldsymbol{z}_k^{(j)})$, for all $i \in [\![1, n_{\mathrm{o}}]\!]$ and all $j \in [\![1, m_k]\!]$.

approximation is investigated numerically in Section V. To simplify the notation, we will omit the time index k in what follows, e.g., we will write $f(\boldsymbol{x}^{(i)} | \boldsymbol{z})$ instead of $f(\boldsymbol{x}_k^{(i)} | \boldsymbol{z}_{1:k})$ and $f(\boldsymbol{x}^{(i)} | \boldsymbol{z}_-)$ instead of $f(\boldsymbol{x}_k^{(i)} | \boldsymbol{z}_{k-1})$.

To develop the proposed LBP method, we first integrate with respect to the target states in (12). In this way, we obtain the following posterior pdf

$$\tilde{p}(\boldsymbol{a}, \boldsymbol{b} | \boldsymbol{z}) \propto \prod_{j=1}^{m} \varphi_j\big(\boldsymbol{b}^{(j)}\big) \prod_{i=1}^{n_{\mathrm{o}}} \psi_{ij}\big(a^{(i)}, \boldsymbol{b}^{(j)}\big) \tag{13}$$

where, for $\boldsymbol{b}^{(j)} = [i, l]$ with $i > l > 0$, we introduce

$$\begin{aligned} \varphi_j\big([i, l]\big) = \frac{\int\int f(\boldsymbol{z}^{(j)} | \boldsymbol{x}^{(i)}, \boldsymbol{x}^{(l)}) Q_{\mathrm{u}}\big(\boldsymbol{x}^{(i)}, \boldsymbol{x}^{(l)}\big)}{\big(1 - P_{\mathrm{d}}^{(i)}\big)\big(1 - P_{\mathrm{d}}^{(l)}\big) \lambda_{\mathrm{c}} f_{\mathrm{c}}\big(\boldsymbol{z}^{(j)}\big)} \\ \times f(\boldsymbol{x}^{(i)} | \boldsymbol{z}_-) f(\boldsymbol{x}^{(l)} | \boldsymbol{z}_-) \mathrm{d}\boldsymbol{x}^{(i)} \mathrm{d}\boldsymbol{x}^{(l)} \end{aligned}$$

and similarly for $\boldsymbol{b}^{(j)} = [i, i]$ with $i \in [\![1, n_{\mathrm{o}}]\!]$, we establish

$$\varphi_j\big([i, i]\big) = \frac{P_{\mathrm{d}}^{(i)} \int f(\boldsymbol{z}^{(j)} | \boldsymbol{x}^{(i)}) f(\boldsymbol{x}^{(i)} | \boldsymbol{z}_-)) \mathrm{d}\boldsymbol{x}^{(i)}}{(1 - P_{\mathrm{d}}^{(i)}) \lambda_{\mathrm{c}} f_{\mathrm{c}}(\boldsymbol{z})}$$

while $\varphi_j([0, 0]) = 1$ and for any other values of $\boldsymbol{b}^{(j)}$ we set $\varphi_j(\boldsymbol{b}^{(j)}) = 0$.

The factorization in (13) lends itself to a message-passing algorithm of the type in [3], [6], [17]. More specifically, we will employ an LBP algorithm that iterates message exchanges between the $\boldsymbol{b}^{(j)}$ and $a^{(i)}$ variables for all $j \in [\![1, m_k]\!]$ and $i \in [\![1, n_{\mathrm{o}}]\!]$. Here, at each iteration, the message from $\boldsymbol{b}^{(j)}$ to $a^{(i)}$ is given by

$$\mu_{\boldsymbol{b}^j \to a^i}(a^i) = \sum_{\boldsymbol{b}^{(j)}} \varphi_j(\boldsymbol{b}^{(j)}) \psi_{ij}(a^{(i)}, \boldsymbol{b}^{(j)}) \prod_{i' \neq i} \mu_{a^{i'} \to \boldsymbol{b}^j}(\boldsymbol{b}^{(j)})$$

while the message from $a^{(i)}$ to $\boldsymbol{b}^{(j)}$ is given by

$$\mu_{a^i \to \boldsymbol{b}^j}(\boldsymbol{b}^{(j)}) = \sum_{a^{(i)}} \psi_{ij}(a^{(i)}, \boldsymbol{b}^{(j)}) \prod_{j' \neq j} \mu_{\boldsymbol{b}^{j'} \to a^i}(a^{(i)}).$$

These messages' values are restricted due to the binary constraints ψ_{ij} in (8). For each $i \in [\![1, n_{\mathrm{o}}]\!]$, let $\mathcal{B}^{(i)} \triangleq \big\{[i, l] \colon l \in$

$[\![1,i]\!]\} \cup \{[l,i]\colon l \in [\![i+1, n_\mathrm{o}]\!]\}$ be the set of all index tuples that contain the i-th target, either solely (via the resolved pair $[i,i]$) or coupled with another target (via an unresolved pair $[l,i]$ for some $l \neq i$). The message $\mu_{\boldsymbol{b}^j \to a^i}$ takes only two distinct values, i.e.,

$$\mu_{\boldsymbol{b}^j \to a^i}(j) = \sum_{\boldsymbol{b}^{(j)} \in \mathcal{B}^{(i)}} \varphi_j(\boldsymbol{b}^{(j)}) \prod_{i' \neq i} \mu_{a^{i'} \to \boldsymbol{b}^j}(\boldsymbol{b}^{(j)})$$

for $a^{(i)} = j$ and

$$\mu_{\boldsymbol{b}^j \to a^i}(t) = \sum_{\boldsymbol{b}^{(j)} \in \mathcal{B} \setminus \mathcal{B}^{(i)}} \varphi_j(\boldsymbol{b}^{(j)}) \prod_{i' \neq i} \mu_{a^{i'} \to \boldsymbol{b}^j}(\boldsymbol{b}^{(j)}) \quad (14)$$

for $a^{(i)} = t \neq j$. Similarly, the message $\mu_{a^i \to \boldsymbol{b}^j}$ also only takes only the two distinct values, i.e.,

$$\mu_{a^i \to \boldsymbol{b}^j}(\boldsymbol{b}^{(j)}) = \prod_{j' \neq j} \mu_{\boldsymbol{b}^{j'} \to a^i}(j)$$

for $\boldsymbol{b}^{(j)} \in \mathcal{B}^{(i)}$ and

$$\mu_{a^i \to \boldsymbol{b}^j}(\boldsymbol{b}^{(j)}) = \sum_{t=0,\, t \neq j}^{m_k} \prod_{j' \neq j} \mu_{\boldsymbol{b}^{j'} \to a^i}(t) \quad (15)$$

for $\boldsymbol{b}^{(j)} \in \mathcal{B} \setminus \mathcal{B}^{(i)}$.

Following [3], [6], [17], one can renormalize each message without affecting the LBP calculations. In particular, by dividing $\mu_{\boldsymbol{b}^j \to a^i}(a^{(i)})$ by (14) and $\mu_{a^i \to \boldsymbol{b}^j}(\boldsymbol{b}^{(j)})$ by (15), we obtain

$$\mu_{\boldsymbol{b}^j \to a^i}(a^{(i)}) \propto \begin{cases} \mu^{ij}_{\boldsymbol{b}a} & \text{if } a^{(i)} = j \\ 1 & \text{otherwise} \end{cases}$$

and

$$\mu_{a^i \to \boldsymbol{b}^j}(\boldsymbol{b}^{(j)}) \propto \begin{cases} \mu^{ij}_{a\boldsymbol{b}} & \text{if } \boldsymbol{b}^{(j)} \in \mathcal{B}^{(i)} \\ 1 & \text{otherwise} \end{cases}$$

where we introduced

$$\mu^{ij}_{\boldsymbol{b}a} = \frac{\varphi_j([i,i]) + \sum_{l>i} \varphi_j([l,i]) \mu^{lj}_{a\boldsymbol{b}} + \sum_{l<i} \varphi_j([i,l]) \mu^{lj}_{a\boldsymbol{b}}}{1 + \sum_{\substack{i'=1 \\ i' \neq i}}^{n_\mathrm{o}} \varphi_j([i',i']) \mu^{i'j}_{a\boldsymbol{b}} + \sum_{\substack{[t,p],t,p \neq i \\ t>p>0}} \varphi_j([t,p]) \mu^{tj}_{a\boldsymbol{b}} \mu^{pj}_{a\boldsymbol{b}}} \quad (16)$$

$$\mu^{ij}_{a\boldsymbol{b}} = \frac{1}{1 + \sum_{\substack{j'=1 \\ j' \neq j}}^{m_k} \mu^{ij'}_{\boldsymbol{b}a}}. \quad (17)$$

The proposed LBP algorithm for the UTT model with generic number of targets n_o proceeds as follows:

1) *initialize* the messages $\mu^{ij}_{a\boldsymbol{b}} = 1 \ \forall i, j$,
2) *update* the messages $\mu^{ij}_{\boldsymbol{b}a}$ via (16) and $\mu^{ij}_{a\boldsymbol{b}}$ via (17) $\forall i, j$,
3) *repeat* previous step as long as the maximum change in messages between subsequent iterations is greater than some fixed threshold (e.g., 10^{-6}) or a maximum number of iterations is reached,
4) *return* final messages $\mu^{ij}_{a\boldsymbol{b}} = 1$.

After LBP has been performed, the estimated association probabilities for all $j \in [\![1, m_k]\!]$ and $\boldsymbol{b}^{(j)} \in \mathcal{B}$ are obtained as

$$\hat{p}_j(\boldsymbol{b}^{(j)}|\boldsymbol{z}) \propto \begin{cases} 1 & \text{if } \boldsymbol{b}^{(j)} = [0,0] \\ \varphi_j([i,i]) \mu^{ij}_{a\boldsymbol{b}} & \text{if } \boldsymbol{b}^{(j)} = [i,i] \\ \varphi_j([i,l]) \mu^{ij}_{a\boldsymbol{b}} \mu^{lj}_{a\boldsymbol{b}} & \text{if } \boldsymbol{b}^{(j)} = [i,l]\,. \end{cases} \quad (18)$$

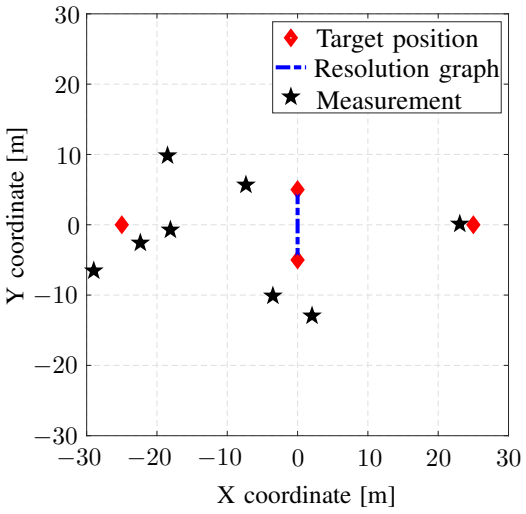

Fig. 2. The first scenario depicts two closely-spaced targets and two well-separated targets. Also, showcasing an instance of the resolution event (or graph) and measurements. The two targets in the middle generate an unresolved measurement with high probability (> 0.6), whereas any other pair of targets has a low probability (< 0.1) of generating unresolved measurements.

Note that the initialization step and each recursion of this LBP algorithm require a number of operations that scales as $O(n_\mathrm{o}^2\, m_k)$.

V. Numerical Evaluation

In this section, we numerically evaluate various algorithms that estimate the marginal association probabilities $p_j(\boldsymbol{b}_k^{(j)}|\boldsymbol{z}_{1:k})$, $\forall\ j \in [\![1, m_k]\!]$ and $\boldsymbol{b}_k^{(j)} \in \mathcal{B}_k$, for the proposed UTT model. More specifically, we showcase the performance of the estimator $\{\hat{p}_j(\cdot|\boldsymbol{z}_{1:k})\}_j$ obtained via the proposed LBP algorithm. This estimator is benchmarked against two exact evaluations of the marginals $\{p_j(\cdot|\boldsymbol{z}_{1:k})\}_j$, obtained via an exhaustive enumeration of all valid joint associations $\boldsymbol{a}_k \in [\![0, m_k]\!]^{n_\mathrm{o}}$ (or equivalently of $\boldsymbol{b}_k \in \mathcal{B}_k$) and marginalizing over their joint probabilities. The two reference methods differ in the way the joint probabilities are evaluated. The first reference method employs the same approximation $V_\mathrm{u}(\boldsymbol{x}_k) \approx$ cst as employed by the LBP method. The resulting marginals of this first reference method are denoted via $\{\tilde{p}_j(\boldsymbol{b}_k^{(j)}|\boldsymbol{z}_{1:k})\}_j$ and represent the exact marginals of the joint association probabilities under assumption $V_\mathrm{u}(\boldsymbol{x}_k) \approx$ cst, i.e., the marginal probabilities that our LBP method aims to compute. The second reference method computes the exact marginals of the joint probabilities $p(\boldsymbol{a}_k|\boldsymbol{z}_{1:k})$, for all $\boldsymbol{a}_k$, without the assumption $V_\mathrm{u}(\boldsymbol{x}_k) \approx$ cst, with the resulting marginals being denoted via $\{p_j(\boldsymbol{b}_k^{(j)}|\boldsymbol{z}_{1:k})\}_j$. These represent the exact marginal association probabilities for the UTT model. Both reference methods require an exhaustive enumeration of all joint association vectors $\boldsymbol{a}_k \in [\![0, m_k]\!]^{n_\mathrm{o}}$ and thus incur a computational complexity of $O((m_k+1)^{n_\mathrm{o}})$.

The Total Variation Distance (TVD) serves as a distance metric between two probability distributions and corresponds to half the L_1 distance between the two probability distributions [20, Ch. 5]. Given pmfs $\hat{p}$ and p defined on the same

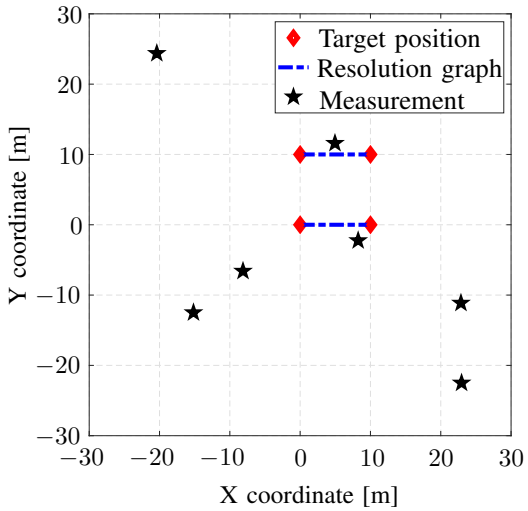

Fig. 3. The second scenario depicts four closely-spaced targets. Also, showcasing an instance of the resolution event (or graph) and measurements. All pairs of targets have a high probability (> 0.6) of generating unresolved measurements .

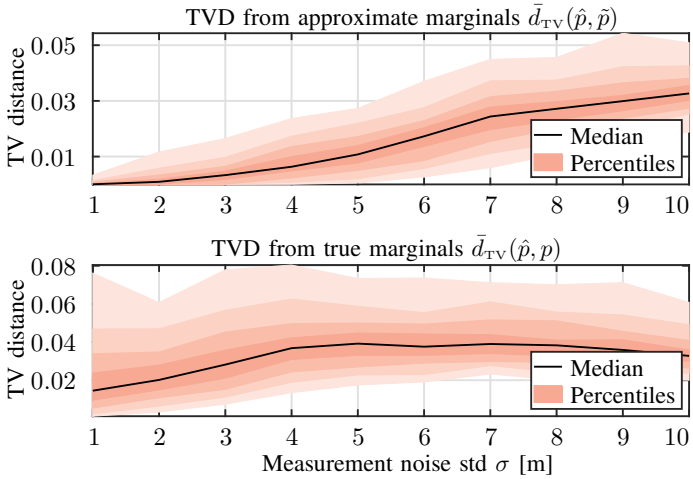

Fig. 4. Total variation distance between the LBP estimated marginals and the exact evaluation of the approximate marginals (upper panel), and exact evaluation of the true marginals (lower panel). The curves correspond to the first scenario and showcase the median error and $10\%-90\%$ percentile bands.

discrete alphabet Ω, the TVD between $\hat{p}$ and p is given by $d_{\text{TV}}(\hat{p}, p) = \frac{1}{2}\sum_{\omega\in\Omega} |\hat{p}(\omega) - p(\omega)|$, with $d_{\text{TV}}(\hat{p}, p) \in [0, 1]$. The TVD distance has the useful interpretation: if, for example, $d_{\text{TV}}(\hat{p}, p) < 0.1$, then the differences in probability between p and $\hat{p}$ are limited to 0.1.

In this work, an average TVD across all measurements is constructed between the LBP estimated marginal association probabilities of (18) and the two reference methods. Specifically, for the first and second reference methods, we construct $\bar{d}_{\text{TV}}(\hat{p}, \tilde{p}) = \frac{1}{m_k}\sum_{j=1}^{m_k} d_{\text{TV}}(\hat{p}_j, \tilde{p}_j)$ and $\bar{d}_{\text{TV}}(\hat{p}, p) = \frac{1}{m_k}\sum_{j=1}^{m_k} d_{\text{TV}}(\hat{p}_j, p_j)$, respectively.

We devise two scenarios with multiple targets that follow the UTT model. The first scenario is presented in Fig. 2 and showcases two closely-spaced targets that generate unresolved targets with high probability and two well-separated targets. This is a relatively mild scenario, where the unresolved phenomenon is mostly restricted to the two targets in the middle. In contrast, Fig. 3 showcases a more difficult scenario where any two targets are highly likely to generate an unresolved measurement. The following parameters are common to both scenarios. The targets follow 2-D Gaussian distributions with means specified in the figures and common covariance matrices $10\,\boldsymbol{I}_2$, where $\boldsymbol{I}_2$ is the 2×2 identity matrix. Resolved measurements consist of noisy versions of target positions with an additive Gaussian noise of covariance matrix $\boldsymbol{R}_k = \sigma^2\,\boldsymbol{I}_2$. Unresolved measurements are noisy versions of the midpoint of the segment formed by the two target positions, with an additive Gaussian noise of covariance matrix $\boldsymbol{R}_k^{\text{u}} = 2\sigma^2\,\boldsymbol{I}_2$. Clutter measurements follow a Poisson point process with a rate of 6 points that are uniformly distributed over the surveillance region of $[-50, 50]^2$. The probability of detection is fixed at 0.9 while unresolved measurements occur according to the UTT model and with a resolution matrix $A_{\text{u}} = 10^2\,\boldsymbol{I}_2$.

Corresponding to the two scenarios, TVD curves as a function of measurement standard deviation (std) σ are presented in Fig. 4 and Fig. 5. The TVD median and percentile intervals (or bands) are obtained by performing 100 independent simulations of the proposed scenarios and methods. The percentile intervals are constructed to gradually incorporate $20\%, 40\%, 60\%$, and 80% of the TVD curves.

As expected, the TVD values increase with increasing σ for both scenarios. Additionally, the TVD cures in both Figs. 4 and 5 showcase slightly higher values for $\bar{d}_{\text{TV}}(\hat{p}, p)$ than for $\bar{d}_{\text{TV}}(\hat{p}, \tilde{p})$. Again, this is to be expected since the proposed LBP algorithm aims to evaluate the marginals of the joint association probability under the assumption $V_{\text{u}}(\boldsymbol{x}_k) \approx$ cst. However, the increase in TVD error is mild throughout the range of σ values, thus justifying the assumption. Numerically, the median TVD cures in all four cases lies under the 0.1 value. This indicates accurate LBP estimates of the marginal association probabilities for the UTT model, despite the ap-

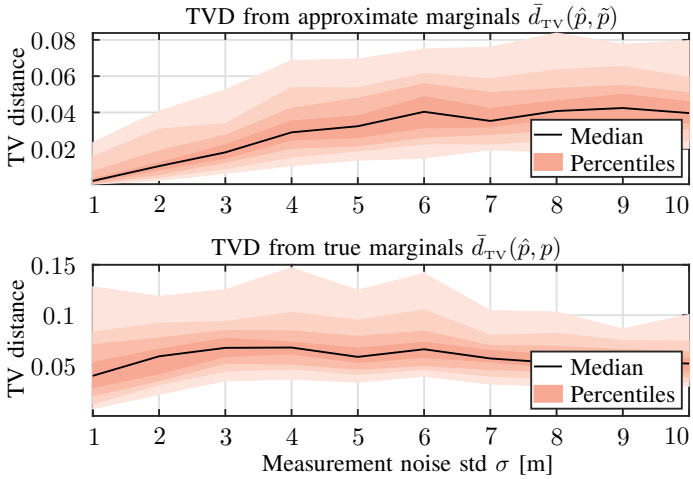

Fig. 5. Total variation distance between the LBP estimated marginals and the exact evaluation of the approximate marginals (upper panel), and exact evaluation of the true marginals (lower panel). The curves correspond to the second scenario and showcase the median error and $10\% - 90\%$ percentile bands.

Number of targets	$n_\mathrm{o}=4$	$n_\mathrm{o}=5$	$n_\mathrm{o}=6$
$\bar{d}_{\mathrm{TV}}(\hat{p},\tilde{p})$	$9.8\mathrm{e}{-3}$	$1.2\mathrm{e}{-2}$	$1.7\mathrm{e}{-2}$
$\bar{d}_{\mathrm{TV}}(\hat{p},p)$	$3.9\mathrm{e}{-2}$	$7.1\mathrm{e}{-2}$	$7.9\mathrm{e}{-2}$
Run time LBP [s]	$7.8\mathrm{e}{-3}$	$1.1\mathrm{e}{-2}$	$1.3\mathrm{e}{-2}$
Run time approx. marginals [s]	$4.2\mathrm{e}{-2}$	$9.1\mathrm{e}{-1}$	16
Run time true marginals [s]	$1.8\mathrm{e}{-1}$	3.8	69

TABLE I
MEAN TVD AND WALL-CLOCK RUN TIMES (IN SECONDS [S]) FOR THE PROPOSED LBP AND REFERENCE METHODS AS A FUNCTION OF THE NUMBER OF TARGETS n_o .

proximation $V_\mathrm{u}(\boldsymbol{x}_k) \approx \text{cst}$. Moreover, the small increase in TVD errors between the two scenarios supports the ability of the proposed LBP method to address cases where a single target is *apriori* equally likely to generate unresolved measurements with several of its neighboring targets.

In Table I, we present the mean TVD values of $\bar{d}_{\mathrm{TV}}(\hat{p},\tilde{p})$ and $\bar{d}_{\mathrm{TV}}(\hat{p},p)$, as well as the mean wall-clock run times of the proposed LBP and the two reference methods. The results in Table I are obtained by averaging over 100 independent simulations on a laptop computer with an Intel $\mathrm{i7}-1255\mathrm{U}$ CPU and 32GB of RAM. The results are presented for different number of closely-spaced targets. The targets are placed at the vertices of a rectangular grid with uniform spacing of 10 m. For example, the first column of the table with $n_\mathrm{o}=4$ corresponds to the scenario in Fig. 3. The explosion of the run time of both reference methods with increasing n_o is caused by the exponential computational complexity $O((m_k+1)^{n_\mathrm{o}})$ required to enumerate all joint associations. The second reference method has a higher run time than the first due to the additional evaluation of $V_\mathrm{u}(\cdot)$, which involves finding all partitions of the set $[\![1,n_\mathrm{o}]\!]$ with subsets of cardinality at most two. In contrast, the LBP provides accurate estimates at a computational cost that only scales as $O(n_\mathrm{o}^2 m_k)$.

VI. CONCLUSION

In this paper, we proposed a method for data association in the presence of unresolved measurements. More specifically, we develop the UTT model and a corresponding LBP algorithm that efficiently approximates the marginal association probabilities given all measurements. The resulting algorithm has quadratic complexity with the number of targets and linear with the number of measurements. It thus offers a scalable solution to the tracking problem under the UTT model. Possible directions for future research include an extension to an unknown number of targets [6], distributed implementations [21], and an enhancement of LBP operations with learned information [22].

ACKNOWLEDGMENT

This work was supported in part by the IP Paris *Centre Interdisciplinaire d'Etudes pour la Défense et la Sécurité* (CIEDS) under the NITSM-MTS project with award no. 2022650059 and in part by the National Science Foundation (NSF) under the CAREER project with award no. 2146261.

REFERENCES

[1] Y. Bar-Shalom and X. R. Li, *Multitarget-Multisensor Tracking: Principles and Techniques*, 2nd ed. Storrs, CT, USA: YBS Publishing, 1995.

[2] A. A. Saucan, T. Chonavel, C. Sintes, and J.-M. Le Caillec, "CPHD-DOA tracking of multiple extended sonar targets in impulsive environments," *IEEE Trans. Signal Process.*, vol. 64, no. 5, pp. 1147–1160, March 2016.

[3] F. Meyer, P. Braca, P. Willett, and F. Hlawatsch, "A scalable algorithm for tracking an unknown number of targets using multiple sensors," *IEEE Trans. Signal Process.*, vol. 65, no. 13, pp. 3478–3493, July 2017.

[4] M. Beard, B. T. Vo, and B. N. Vo, "Bayesian multi-target tracking with merged measurements using labelled random finite sets," *IEEE Trans. Signal Process.*, vol. 63, no. 6, pp. 1433–1447, Mar. 2015.

[5] A. A. Saucan, M. J. Coates, and M. Rabbat, "A multisensor multi-Bernoulli filter," *IEEE Trans. Signal Process.*, vol. 65, no. 20, pp. 5495–5509, October 2017.

[6] F. Meyer, T. Kropfreiter, J. L. Williams, R. Lau, F. Hlawatsch, P. Braca, and M. Z. Win, "Message passing algorithms for scalable multitarget tracking," *Proc. IEEE*, vol. 106, no. 2, pp. 221–259, February 2018.

[7] B.-N. Vo, B.-T. Vo, and D. Phung, "Labeled random finite sets and the Bayes multi-target tracking filter," *IEEE Trans. Signal Process.*, vol. 62, no. 24, pp. 6554–6567, Dec. 2014.

[8] A. A. Saucan and M. Z. Win, "Information-seeking sensor selection for ocean-of-things," *IEEE Internet Things J.*, vol. 7, no. 10, pp. 10 072–10 088, October 2020, special issue on *Internet of Things for Smart Ocean*.

[9] K.-C. Chang and Y. Bar-Shalom, "Joint probabilistic data association for multitarget tracking with possibly unresolved measurements," in *American Control Conference*, 1983, pp. 466–471.

[10] ——, "Joint probabilistic data association for multitarget tracking with possibly unresolved measurements and maneuvers," *IEEE Trans. Autom. Control*, vol. 29, no. 7, pp. 585–594, 1984.

[11] ——, "A simplification of the JPDAM algorithm," *IEEE Trans. Autom. Control*, vol. 31, no. 10, pp. 989–991, 1986.

[12] W. Koch and G. Van Keuk, "Multiple hypothesis track maintenance with possibly unresolved measurements," *IEEE Trans. Aerosp. Electron. Syst.*, vol. 33, no. 3, pp. 883–892, 1997.

[13] S. Jeong and J. K. Tugnait, "Tracking of two targets in clutter with possibly unresolved measurements," *IEEE Trans. Aerosp. Electron. Syst.*, vol. 44, no. 2, pp. 748–765, 2008.

[14] R. B. Angle, R. L. Streit, and M. Efe, "Multiple target tracking with unresolved measurements," *IEEE Signal Process. Lett.*, vol. 28, pp. 319–323, 2021.

[15] D. Svensson, M. Ulmke, and L. Hammarstrand, "Multitarget sensor resolution model and joint probabilistic data association," *IEEE Trans. Aerosp. Electron. Syst.*, vol. 48, no. 4, pp. 3418–3434, Oct. 2012.

[16] A. A. Saucan and M. Z. Win, "On the labeled multi-Bernoulli filter with merged measurements," in *IEEE Int. Conf. Commun.*, 2020, pp. 1–5.

[17] J. Williams and R. A. Lau, "Approximate evaluation of marginal association probabilities with belief propagation," *IEEE Trans. Aerosp. Electron. Syst.*, vol. 50, no. 4, pp. 2942–2959, 2014.

[18] F. Meyer and J. L. Williams, "Scalable detection and tracking of geometric extended objects," *IEEE Trans. Signal Process.*, vol. 69, pp. 6283–6298, February 2021.

[19] F. R. Kschischang, B. J. Frey, and H.-A. Loeliger, "Factor graphs and the sum-product algorithm," *IEEE Trans. Inf. Theory*, vol. 47, no. 2, pp. 498–519, February 2001.

[20] L. Devroye and G. Lugosi, *Combinatorial Methods in Density Estimation*. New York, NY: Springer, 2001.

[21] P. Sharma, A. A. Saucan, D. J. Bucci, and P. K. Varshney, "Decentralized Gaussian filters for cooperative self-localization and multi-target tracking," *IEEE Trans. Signal Process.*, vol. 67, no. 22, pp. 5896–5911, November 2019.

[22] M. Liang and F. Meyer, "Neural enhanced belief propagation for multiobject tracking," *IEEE Trans. Signal Process.*, 2023, to appear.